The NMR MOUSE, a Mobile Universal Surface Explorer

G. EIDMANN, R. SAVELSBERG, P. BLÜMLER, AND B. BLÜMICH*

Institut für Makromolekulare Chemie, RWTH Aachen, D-52074 Aachen, Germany

A mobile NMR surface scanner has been developed for the nondestructive investigation of arbitrarily large objects. While RF generation and pulse programs are controlled by a PC-based NMR console, the probe provides not only the B_1 RF field but also the static B_0 polarization field. Because of its compactness and mobility, the apparatus was named NMR MOUSE for *mo*bile *u*niversal *s*urface *e*xplorer.

NMR imaging has been proven to be a useful tool not only in clinical diagnostics but also in materials science (*1, 2*). Its advantages, given by its noninvasiveness and the variety of NMR parameters which can be correlated with material properties, are offset by the restrictions in sample size due to the limited volume of superconducting magnets and, especially in solids, in the size of RF coils (*3*). Small coils are required for generation of strong RF fields to cope with strong spin interactions and to fit MAS rotors. Surface coils (*4–6*) with their inhomogeneous B_1 field exhibit a high filling factor and reduce the spatial limitations, but are usually used in a homogeneous B_0 field of limited volume. To overcome the spatial limitations, more-open magnet designs were first introduced in medical science (*7*), but without mobile service. Thus a mobile NMR device would dramatically increase the possibilities of NMR investigations in materials science, process and quality control, biology, environmental science, and medicine.

One example of the use of compact and mobile NMR spectrometers with open geometries is oil-well logging in the mineral-oil industry (*8*). Kleinberg and co-workers (*9*) have developed a dedicated NMR spectrometer, which fits into a drill hole and can be used on the rig. It produces a relatively homogeneous B_0 field normal to the probe in the surrounding rock a few centimeters away from the probe, and a semi-coaxial RF antenna is used for excitation and detection. Suitable pulse sequences were developed for multiparameter analysis of fluids in rock pores (*10, 11*). From the relaxation and the restricted diffusion in such pores relevant geologic information can be derived.

Similar methods with a restricted sensitive area are the early FONAR (*12*) method and the more recently developed ''stray-field imaging'' or STRAFI method (*13*). In the latter,

the extremely strong B_0 gradients in the stray fields of superconducting magnets restrict the excited volume of an RF pulse to a slice only a few micrometers thick. By mechanical movement of the sample through this sensitive plane projections as well as 2D and 3D images can be obtained. Most recently, Miller and Garroway (*14, 15*) combined the STRAFI technique with the use of surface coils, and in this way demonstrated that NMR signals can be measured by an inhomogeneous B_1 field perpendicular to an inhomogeneous B_0 field. Because their experiments were performed at the lower end of a superconducting magnet, relatively large objects could be scanned.

The basic experimental setup of the surface scanner we constructed is shown in Fig. 1a. The generation of the RF pulses, their amplification, and signal detection are done by
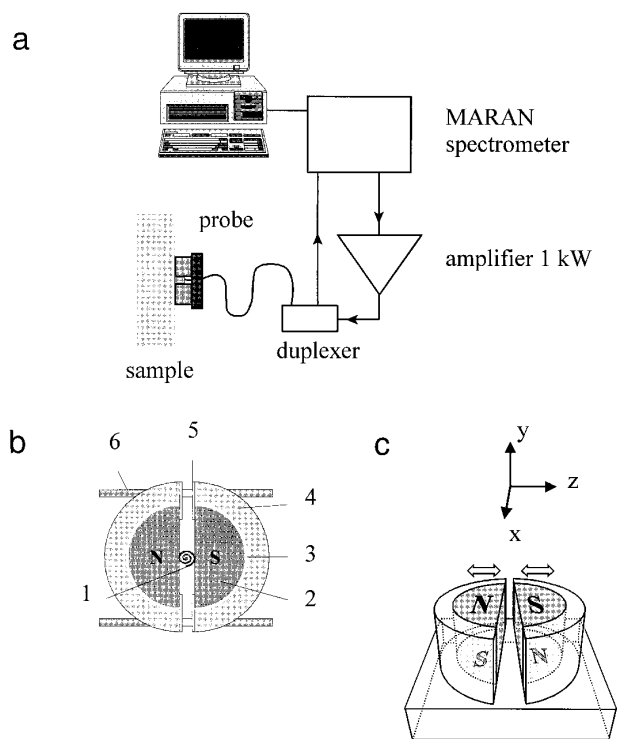
FIG. 1. Setup of the NMR MOUSE: (a) spectrometer and (b, c) probe design.

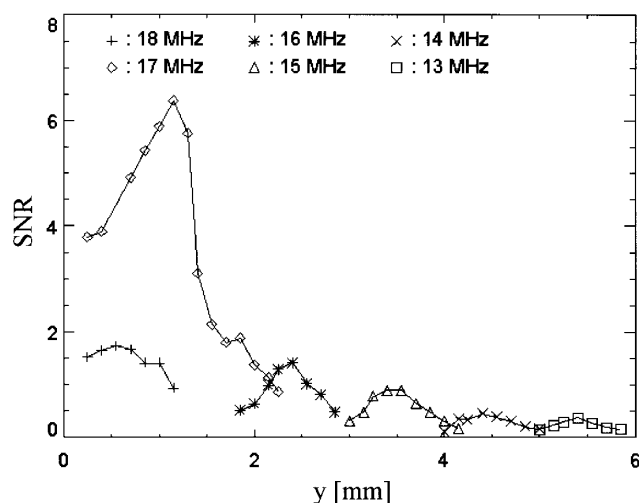* To whom correspondence should be addressed.

FIG. 2. SNR versus Larmor frequency and depth.

a commercial low-field (1 to 64 MHz) NMR spectrometer (Maran) from Resonance Instruments Ltd. (Witney, UK). The spectrometer is controlled by a standard desktop PC. The setup has been completed by a duplexer from Bruker and a broadband 1 kW amplifier from AMT usually driven in a power range from 100 to 300 W. The entire prototype setup fits into a standard computer desk, so that it can easily be transported to the objects to be investigated.

The pulse programs are written in Turbo Pascal (Borland) implementing the original control modules from Resonance Instruments. The NMR signals are acquired in quadrature. They can be displayed and stored by the PC. Further data analysis is done using ORIGIN and a special NMR library (16) for PV-WAVE from Visual Numerics.

The B_0/B_1 probe weighs about 2.5 kg and can be positioned manually on the surfaces of arbitrarily large objects. It consists of two permanent magnets embedded in an iron yoke, which are separated by a small gap of 13 mm width where the RF coil (1) is located (Fig. 1b). The permanent magnets (2) are of a semicylindrical shape, 31 mm in height and 55 mm in diameter, made of an NdFeB alloy (17). They are axially magnetized and placed face to face with antiparallel magnetization (Fig. 1c). The magnetic field is mostly parallel to the plane surface of the magnets and assumes a maximum at their surface of about 0.5 T. The round surfaces of the magnets are covered by a 1 mm thick PTFE layer (3) and surrounded by 10 mm strong iron parts (4) to form a yoke. Each magnet is held in place by two aluminum plates (5) mounted on the iron parts (4). The iron yoke is completed by a 10 mm thick iron plate at the base (Fig. 1c), so that the magnetic field at the top of the gap is increased. The gap between the two magnets can be adjusted by two bolts with opposite threads (6) in a range from 6 to 20 mm (Fig. 1b).

The RF coil is a four-layer solenoid with eight turns per layer. It was made from copper wire with a diameter of 0.5 mm and is embedded in proton-free cement (18). Its dimensions are $13 \times 13 \times 10$ mm, and its inductance is of the order of 3 μH. To achieve a maximum sensitive volume, its axis points perpendicular to the surface of the scanner and aligns with the surface of the magnets. The tuning and matching capacities are located in a shielded case below the iron base plate. With such a straightforward design, deadtimes of about 10 μs could be reached. Because of the inhomogeneous $\mathbf{B}_1$ and $\mathbf{B}_0$ fields, single- and multiecho techniques such as Hahn echoes, CPMG (19), and OW4 [multiple solid echoes (20)] are employed. Due to the depth dependence of the excitation flip angle, it is not a priori clear if the maximum signal originates from CPMG or OW4 excitation or from some angle intermediate between 90° and 180° for echo refocusing.
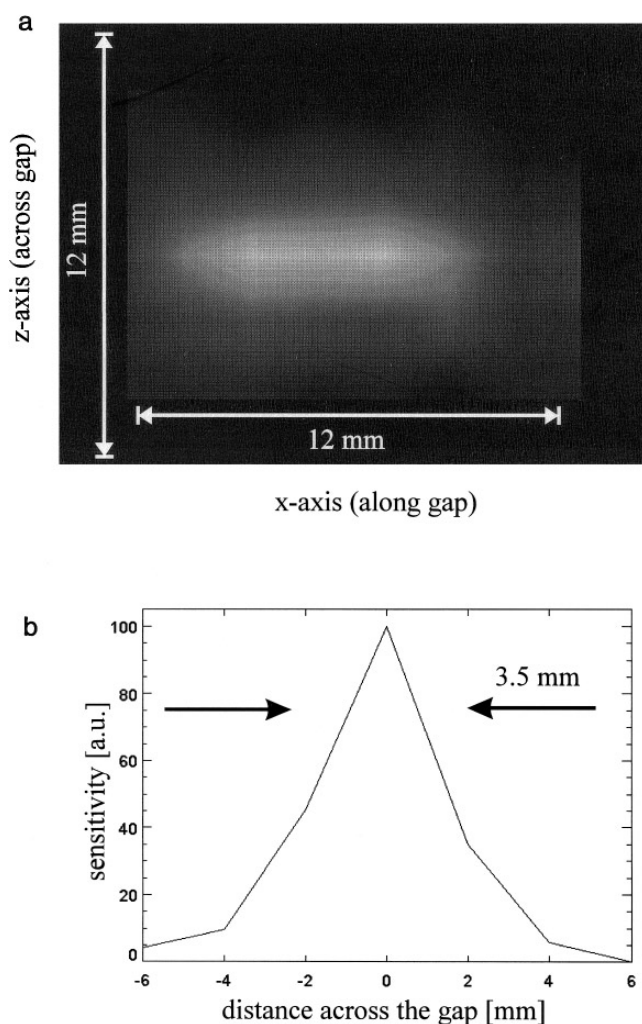

FIG. 3. (a) Signal amplitude as a measure of the lateral spatial resolution in the xz plane at 17 MHz (abscissa, x direction along the gap; ordinate, z direction across the gap) and (b) average along the gap (x direction) versus z direction (across the gap).

TABLE 1
Signal-to-Noise Ratios (SNR) of Various Samples

| Sample	Signal (corrected)	Noise	Signal-to-noise ratio (corrected)
PS	484	42.9	11.3
PC	1,682	58.5	28.8
HDPE	1,138	23.2	49.1
PMMA	1,167	49.0	23.8
SBR	13,270	22.6	587.2
PDMS	14,908	27.9	534.3
Latex glove	13,529	35.4	382.2
Tire	11,842	44.0	269.1
Apple	2,986	46.4	64.4
Chocolate	4,503	18.8	239.5
Walnut kernel	7,387	28.7	257.4
Cheese	10,365	28.2	367.6
Noodle (raw)	2,211	65.0	34.0
Potato (raw)	8,112	50.1	161.9
Wood	912	59.2	15.4
Paper	580	43.0	13.5
Roofing felt (bitumen)	4,379	49.4	88.6
Soap	3,290	29.4	111.9
Human hand	7,379	124.5	59.3
Empty	407	30.4	13.4

Note. For all samples, Hahn-echo-type sequences were used. The SNRs are given for the accumulation of 1024 scans, an echo time τ of 50 μs at 17 MHz, an RF power of about 160 W, and a duration of 2 μs for the refocusing pulses. For determining the signal amplitude, the background signal has been subtracted from the sample signals.

To describe the depth resolution of the probe, the signal-to-noise ratio (SNR) of a thin latex layer (0.5 $\times$ 20 $\times$ 20 mm) was measured as a function of frequency and depth (Fig. 2). Its distance to the coil surface was varied with the help of glass spacers. In the Hahn-echo-type pulse sequence, the pulse length was 2 μs for the refocusing pulses. The pulse separation was $\tau = 100$ μs and the recycling delay was 50 ms. With RF powers of a few hundred watts, depending on the circuit tuning at a given frequency, the optimum pulse angle for each distance was determined from the signal-response maximum.

As can be seen from Fig. 2, the probe is most sensitive at a Larmor frequency of about 17 MHz. This frequency corresponds to a depth range of 0–2 mm. To characterize the lateral spatial resolution at this frequency, a latex-filled glass cylinder (15 mm long, 3.5 mm inner diameter) was moved over a region of 12 $\times$ 12 mm and the signal intensity was determined at each position (Fig. 3a) using a two-pulse Hahn-echo-like sequence. The pulse length for the refocusing pulse was 2 μs at 190 W RF power. The sensitive region forms a narrow strip of about 3.5 mm half-width along the symmetry axis of the gap. For the sensitivity profile across the gap the average along the gap was taken (Fig. 3b). The relatively small sensitivity at the rim of the gap is explained by $\mathbf{B}_1$ field deterioration due to eddy currents induced in the permanent magnets.

To demonstrate the application potential of the NMR MOUSE, various proton-containing samples have been investigated. A signal can be measured from almost any soft or rigid solid. A collection of SNR values of a variety of samples is given in Table 1. Some examples for investigations of material from synthetic polymers are given in the following.

The degree of strain in a household rubber band was measured over a range of $\lambda = L/L_0 = 1$ to $\lambda = 6.25$ using an OW4-type sequence of 400 echoes with a pulse length of 1 μs and a pulse spacing of $\tau = 25$ μs. For each echo 30 data points were acquired with a dwell time 0.5 μs. The recycle delay was set to 250 ms, and 8192 scans were accumulated. The time constants T_{2e} of the biexponential decay of the echo amplitudes were determined for each value of the elon-
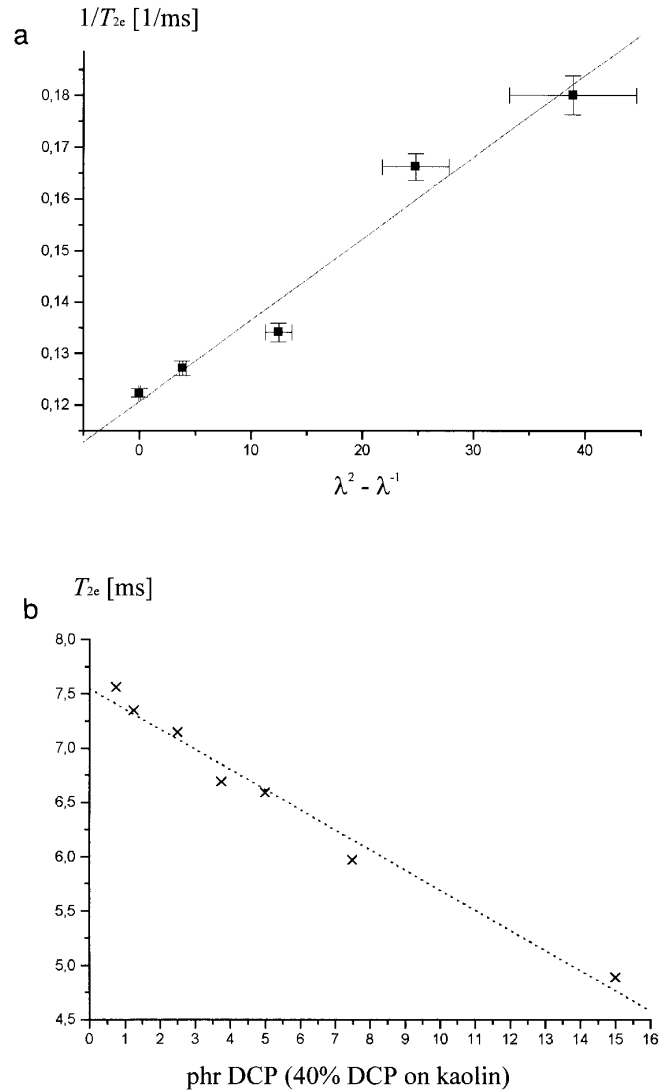
FIG. 4. Examples for the dependence of T_{2e} with material properties: (a) strain and (b) cross-link density.
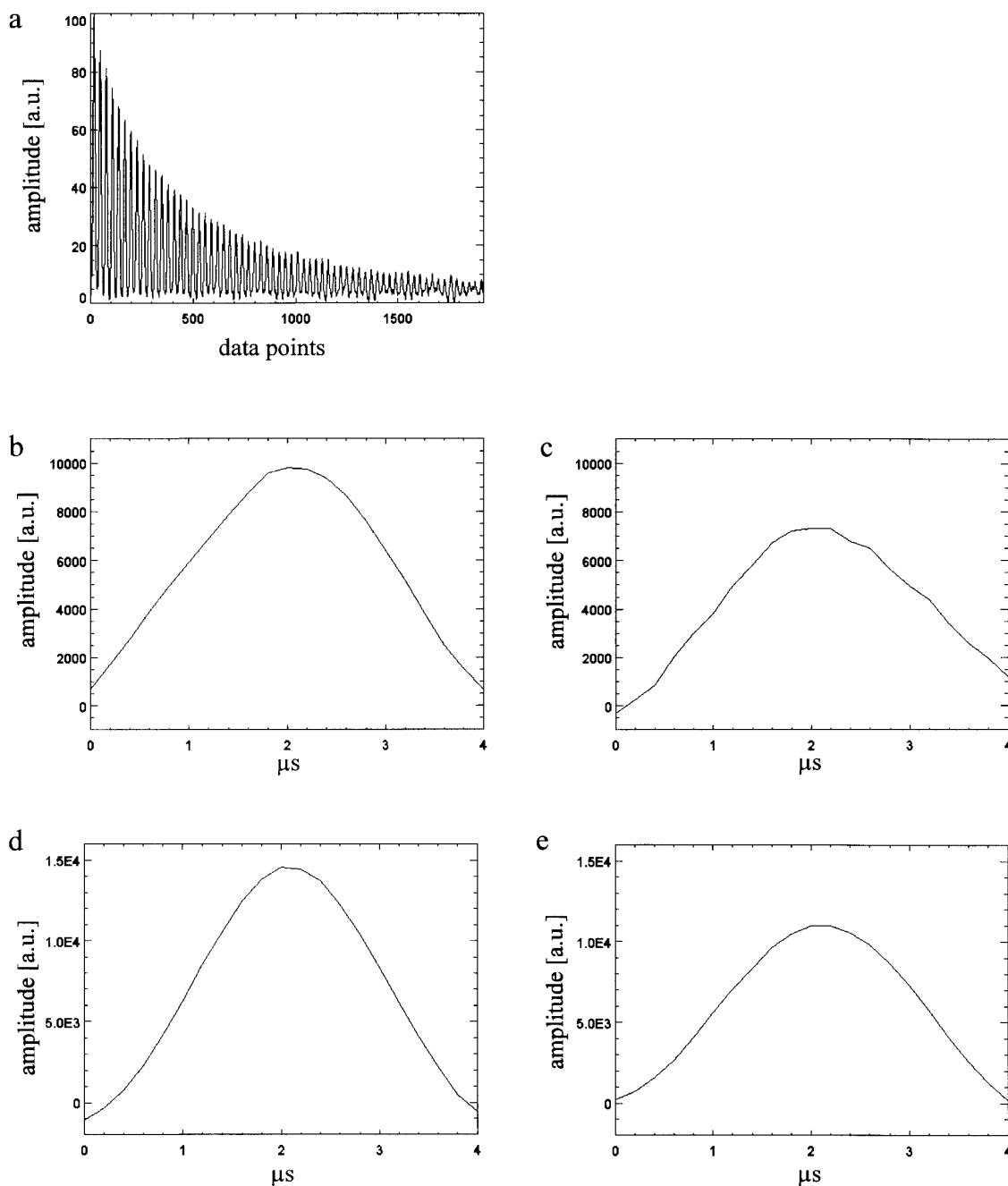
FIG. 5. (a) CPMG-type echoes from a steel-belted tire tread. Acquisition data: 64 echoes with 30 data points each, 0.5 μs dwell time, 2 μs refocusing pulse length, τ of 100 μs, 1 s recycle delay, and 8192 scans (a, b, c) and 1024 scans (d, e), respectively. After 800 μs, the Hahn-type echoes (c, e) are compared with the CPMG echoes (b, d). The signals from the tire tread (b, c) are weaker than the signals from the sidewall (d, e), and the Hahn-type echoes (c, e) are lower than the corresponding CPMG-type echoes (b, d).

gation λ. An apparently linear correlation between the relaxation rate $1/T_{2e}$ of the slow component on the elongation $\lambda^2 - \lambda^{-1}$ is observed (Fig. 4a).

Furthermore, the cross-link density of differently vulcanized NR samples was examined by the relaxation time T_{2e} of the slow component (Fig. 4b) by fitting a biexponential function for the experimentally determined multiecho decay.

Again an apparently linear relation between T_{2e} and cross-link density in terms of the concentration of the peroxidic cross-linker (dicumyl peroxide, DCP) was observed. This concentration is known to scale in proportion with the cross-link density. Thus the scanner can be used to monitor cross-link density in vulcanized rubbers.

It is interesting to note that entire steel-belted car tires

can be investigated by the NMR MOUSE. Depending on the orientation of the steel belts with respect to the magnet gap of the scanner probe, the steel in the sample acts like a yoke and may even homogenize the magnetic field in the sensitive region. This is observed in terms of broader echoes from the tire tread near the steel belt (Figs. 5b, 5c) as compared to the narrower echoes from the sidewall (Figs. 5d, 5e). In the same figure, echo amplitudes are compared for multiecho excitation of the CPMG type and two-pulse echoes of the Hahn type. For identical echo times, the two-pulse echoes (c, e) are lower in amplitude than the echoes from the multiecho train (b, d). Because particle diffusion is ineffective in cross-linked rubbers on the given time scale, this proves that there is a line-narrowing effect associated with the multiecho excitation similar to the line-narrowing effect of the OW4 sequence. Similar line-narrowing effects have been observed with surface coils in homogeneous $\mathbf{B}_1$ fields (21).

An example of the applicability of the NMR MOUSE to rigid polymers is the detection of material change in polystyrene (PS). A circular sheet of impact-modified PS (60 mm diameter, 1 mm thick) was bent to evoke stress whitening. By optical inspection, the stress whitening occurred in a 5 mm wide strip across the sheet diameter. The sample was scanned with a multiecho pulse sequence in a pointwise fashion along a diameter orthogonal to the strip of stress whitening. A typical signal from the unaffected part of the sample is depicted in Fig. 6a. The decay is at least biexponential: For echo times up to 200 μs a background signal of protons inside the coil is predominant while the actual signal from the sample makes up the remaining part. A plot of the latter time constant along the scanned diameter of the PS sheet exhibits an approximately symmetrical behavior relative to the center of the gap at $z = 0$ (Fig. 6b). The T_{2e} values differ significantly for the affected and the unaffected regions. Thus rigid polymers can be investigated as well with the NMR MOUSE, benefiting from line-narrowing effects of multiecho excitation.

These experiments demonstrate that restrictions in sample size to fit conventional NMR spectrometers and imagers can be overcome by use of surface techniques, where both the $\mathbf{B}_0$ and the $\mathbf{B}_1$ fields are applied locally to the object. Excitation and detection of the signal are restricted to regions close to the surface of the object. For the given prototype of the scanner the depth penetration is 5 mm. Although spectroscopic information cannot be acquired in such inhomogeneous fields, relaxation times are sensitive to material properties like stress and cross-link density in elastomers and stress whitening in rigid polymers. Line-narrowing effects from multipulse excitation promise applicability of the surface scanner to a wide range of solid objects. More detailed investigations with regard to probe optimization, pulse excitation schemes, and applications are in progress.
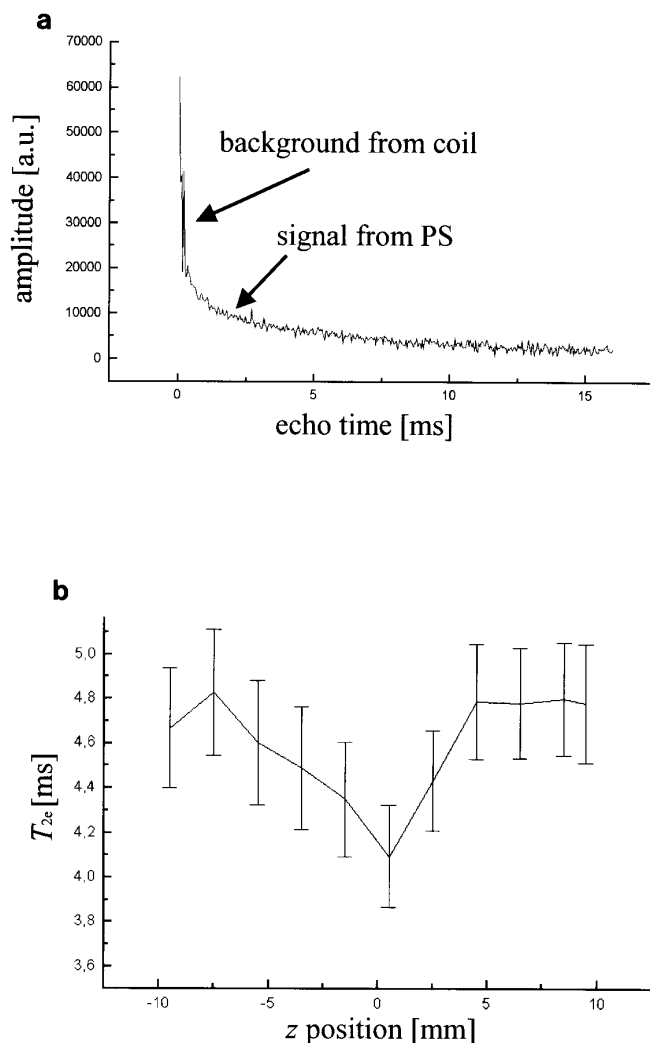
FIG. 6. (a) Typical decay of the echo amplitudes in an OW4 sequence and (b) variation of T_{2e} for different positions of the NMR MOUSE across the PS sample.

REFERENCES

1. B. Blümich and W. Kuhn (Eds.), ''Magnetic Resonance Microscopy: Methods and Applications in Materials Science, Agriculture, and Biomedicine,'' VCH Publishers, Weinheim, 1992.

2. P. T. Calaghan, ''Principles of Nuclear Magnetic Resonance Microscopy,'' Clarendon Press, Oxford, 1991.

3. D. G. Cory, *Annu. Rep. NMR* 24, 87 (1992).

4. D. I. Hoult and R. E. Richards, *J. Magn. Reson.* 24, 71 (1976).

5. J. J. H. Ackerman, *Conc. Magn. Reson.* 2, 33 (1990).

6. J. J. H. Ackerman, T. H. Grove, G. G. Wong, D. G. Gadian, and G. K. Radda, *Nature* 283, 167 (1980).

7. H. Morneburg (Ed.), ''Bildgebende Systeme für die Medizinische Diagnostik,'' p. 514, MCD-Verlag, Erlangen, 1995, and references therein.

8. J. A. Jackson, *J. Magn. Reson.* 41, 411 (1980).

9. R. L. Kleinberg, A. Sezginer, D. D. Griffin, and M. Fukuhara, *J. Magn. Reson.* 97, 466 (1992).

10. L. L. Latour, R. L. Kleinberg, and A. Sezginer, *J. Colloid Interface Sci.* 150, 535 (1992).

11. R. L. Kleinberg, C. Straley, W. E. Kenyon, R. Akkurt, and S. A. Farooqui, *Soc. Petrol. Eng.,* Paper 26470 (1993).

12. R. Damadian, M. Goldsmith, and L. Minkoff, ''NMR 19, NMR in Medicine,'' Springer-Verlag, Heidelberg, 1981.

13. A. A. Samoilenko, D. Y. Artemov, and L. A. Sibeldina, *JETP Lett.* 47, 348 (1988).

14. J. B. Miller and A. N. Garroway, 35th Experimental NMR Conference, Pacific Grove, California, p. 186, 1994.

15. J. B. Miller, Naval Research Laboratory, Washington, DC, private communication.

16. P. Blümler, ''NMR WAVE Library,'' available at http://www.mc.rwth-aachen.de/nmr/nmr.html.

17. VACODYM 370 HR, Dexter Magnetic Materials GmbH, Planegg, Germany.

18. Sauereisenzement No. 8, Sepp Zeug KG, Böblingen-Tannenberg, Germany.

19. S. Meiboom and D. Gill, *Rev. Sci. Instrum.* 29(8), 688 (1958).

20. E. D. Ostroff and J. S. Waugh, *Phys. Rev. Lett.* 16, 1097 (1966).

21. J. B. Miller and A. N. Garroway, *J. Magn. Reson.* 77, 187 (1988).